

UDC 539.1

Microscopic description of ${}^8\text{Li}$ and ${}^8\text{B}$ nuclei within three-cluster model

Vasilevsky V.S.^{1*}, Takibayev N.Zh.², Duisenbay A.D.²

¹*Bogolyubov Institute for Theoretical Physics, 14-B, Metrolohichna str., Kiev, 03680, Ukraine*

²*Department of Physics and Technology, al-Farabi Kazakh National University,
71 al-Farabi av., 050040 Almaty, Kazakhstan*

e-mail: vsvasilevsky@gmail.com

We make theoretical analysis of bound and resonance states of ${}^8\text{Li}$ and ${}^8\text{B}$ nuclei. The analysis is carried out within a three-cluster microscopic model which account for polarizability of interacting clusters. Main attention is paid to the nature of resonances states embedded in two-cluster continuum. We also study effects of the cluster polarization on the spectrum of bound and resonance states, and on the elastic and inelastic $n + {}^7\text{Li}$ and $p + {}^7\text{Be}$ scattering.

Key words: Cluster model, polarization, resonance state.

PACS number(s): 24.10.-i, 21.60.Gx

1 Introduction

Analysis of the astrophysical data on the abundance of light atomic nuclei in the Universe stimulated new and more detail experimental and theoretical investigations of reactions induced by interaction of light nuclei. For the astrophysical applications one has to know the cross section of a reaction at the low energy region, which amounts several kiloelectron volts in the entrance channel of the reaction. This region of energy can be easily achieved at experimental facilities for the reactions induced by interaction of neutrons with light nuclei. However, it is not the case for interaction of light nuclei, containing one or more protons. Coulomb interaction between nuclei makes very difficult to measure the cross section. In this case theoretical methods are invaluable tool to determine or to evaluate the cross section of importance.

As many of light nuclei are weakly bound, they could easy change their size or shape while interacting with neutrons, protons or other light nuclei. This phenomenon is called the polarization. A microscopic three-cluster model was formulated in Ref. [1] to take into account polarizability of the interacting clusters. We refer to it as "cluster polarization". It was shown in Refs [1 – 4] that cluster polarization plays an important role in formation of bound and resonance states in seven nucleon systems. It was also shown that cluster polarization has large impact on different types of reactions in ${}^7\text{Li}$ and ${}^7\text{Be}$ nuclei. Within the present paper, the effects of cluster polarization will be studied in light mirror nuclei ${}^8\text{Li}$ and ${}^8\text{B}$, and

interaction of neutron with ${}^7\text{Li}$ and proton with ${}^7\text{Be}$. Both ${}^7\text{Li}$ and ${}^7\text{Be}$ nuclei have well established two-cluster structure: ${}^4\text{He} + {}^3\text{H}$ and ${}^4\text{He} + {}^3\text{He}$, respectively. This fact is taken into account in the present model. We are also going to consider bound and resonance states of the mirror nuclei ${}^8\text{Li}$ and ${}^8\text{B}$ within three-cluster microscopic model. We study resonance states created by two-cluster and three-cluster configurations.

Properties of mirror nuclei ${}^8\text{Li}$ and ${}^8\text{B}$ have been intensively investigated in microscopic and semimicroscopic models. Besides different experimental methods were used to determine structure of ${}^8\text{Li}$ and ${}^8\text{B}$ and nuclear reactions in these nuclei. In particular, new resonance states of ${}^8\text{B}$ have been recently discovered in [5, 6] in elastic ${}^7\text{Be} + p$ scattering.

The novelty of our approach is that it allows us to consider cluster polarizations. It means that within the proposed model, size and shape of clusters are not fixed but depend on distance between interacting clusters. In the present case we consider how size of ${}^7\text{Li}$ (${}^7\text{Be}$) is changed when neutron (proton) moves toward ${}^7\text{Li}$ (${}^7\text{Be}$).

2 Method and model space

We shall consider ${}^8\text{Li}$ as a three-cluster configuration ${}^8\text{Li} = \alpha + t + n$ and nucleus ${}^8\text{B}$ we shall represent as the configuration ${}^8\text{B} = \alpha + {}^7\text{He} + p$. These configurations are dynamically distinguished from other three-cluster configurations as they have minimal threshold energy compared to other three-cluster configurations in ${}^8\text{Li}$ and ${}^8\text{B}$. By using

such three-cluster configurations we can take into account the following set of two-cluster channels: ${}^7\text{Li} + n$, ${}^5\text{He} + {}^3\text{He}$, ${}^4\text{He} + {}^4\text{He}$ in ${}^8\text{Li}$ and ${}^7\text{Be} + p$, ${}^5\text{Li} + {}^3\text{He}$, ${}^4\text{Li} + {}^4\text{He}$ in ${}^8\text{B}$. Moreover, with such three-cluster configurations, we can consider nuclei ${}^7\text{Li}$, ${}^5\text{He}$, ${}^4\text{H}$, ${}^7\text{Be}$, ${}^5\text{Li}$, ${}^4\text{Li}$ as two-cluster systems: ${}^7\text{Li} = \alpha + t$, ${}^5\text{He} = \alpha + n$, ${}^4\text{He} = t + n$, ${}^7\text{Be} = \alpha + {}^3\text{He}$, ${}^5\text{Li} = \alpha + p$, ${}^4\text{Li} = {}^3\text{He} + p$ and provide more advanced description of internal structure of these nuclei.

$$\Psi_{E_{\alpha} J_{\alpha}}^{(\alpha)} = \widehat{\mathcal{A}}_{\beta\gamma} \left\{ \left[\Phi_{\beta}(A_{\beta}, s_{\beta}) \Phi_{\gamma}(A_{\gamma}, s_{\gamma}) \right]_{S_{\alpha}} g_{\lambda_{\alpha} l_{\alpha}}^{(E)}(x_{\alpha}) Y_{\lambda_{\alpha}}(\hat{\mathbf{x}}_{\alpha}) \right\}_{J_{\alpha}} \quad (1)$$

Indexes α , β and γ form cyclic permutations of 1, 2 and 3.

Wave function of discrete and continuous spectrum states of three-cluster system is

$$\Psi_{E,J} = \sum_{\alpha=1}^3 \widehat{\mathcal{A}} \left\{ \left[\Phi_1(A_1, s_1) \Phi_2(A_2, s_2) \Phi_3(A_3, s_3) \right]_S \times f_{\lambda_{\alpha} l_{\alpha}, L}^{(E,J)}(x_{\alpha}, y_{\alpha}) \left\{ Y_{\lambda_{\alpha}}(\hat{\mathbf{x}}_{\alpha}) Y_{l_{\alpha}}(\hat{\mathbf{y}}_{\alpha}) \right\}_L \right\}_J \quad (2)$$

where $\Phi_{\alpha}(A_{\alpha}, s_{\alpha})$ is a many-particle shell-model wave function describing the internal motion of cluster α ($\alpha = 1, 2, 3$), consisted of A_{α} nucleons ($1 \leq A_{\alpha} \leq 4$), and s_{α} denotes spin of the cluster.

Similarly to the case of three particles, we use three Faddeev amplitudes $f_{\lambda_{\alpha} l_{\alpha}, L}^{(E,J)}(x_{\alpha}, y_{\alpha})$ and three sets of the Jacobi coordinates \mathbf{x}_{α} and \mathbf{y}_{α} . The Jacobi coordinates determine relative position of the center of mass of three clusters. In our notations, \mathbf{x}_{α} is the Jacobi vector, proportional to the distance between β and γ clusters, while \mathbf{y}_{α} is a Jacobi vector connecting the α cluster to the center of mass of the β and γ clusters. Vectors $\hat{\mathbf{x}}_{\alpha}$ and $\hat{\mathbf{y}}_{\alpha}$ denotes unit vectors $\hat{\mathbf{x}}_{\alpha} = \mathbf{x}_{\alpha} / |\mathbf{x}_{\alpha}|$ and $\hat{\mathbf{y}}_{\alpha} = \mathbf{y}_{\alpha} / |\mathbf{y}_{\alpha}|$. Antisymmetrization operators $\widehat{A}_{\beta\gamma}$ and \widehat{A} make antisymmetric wave functions of two- and three-cluster systems, respectively. Note that shell-model wave functions $\Phi_{\alpha}(A_{\alpha}, s_{\alpha})$ are antisymmetric, thus operator $\widehat{A}_{\beta\gamma}$ and \widehat{A} permute nucleons from different clusters.

Note that the shell-model wave function $\Phi_{\alpha}(A_{\alpha}, s_{\alpha})$ explicitly depends on oscillator length b . In different realizations of the many-cluster model this parameter is used as a variational or adjustable parameter. As a rule oscillator length is adjusted to minimize bound state energy of clusters or to reproduce their size (i.e. mass or proton root-mean-square (rms) radius). Within all our models we use common oscillator length for all clusters involved in calculations.

To describe selected three-cluster configurations we employ Algebraic Model with Gaussian and Oscillator Basis (AMGOB) [1 – 4]. We start with construction of wave functions for two-cluster subsystems and for compound three-cluster system. Two-cluster wave function $\Psi_{J_{\alpha}}^{(\alpha)}$, describing interaction of clusters with indexes β and γ , can be written as

The Faddeev amplitudes $f_{\lambda_{\alpha} l_{\alpha}, L}^{(E,J)}(x_{\alpha}, y_{\alpha})$ in eq. (2) is marked by two partial orbital momenta λ_{α} and l_{α} . They are associated with the Jacobi vectors \mathbf{x}_{α} and \mathbf{y}_{α} , respectively. In what follows we assumethat λ_{α} is the orbital momentum of two-cluster subsystem and l_{α} is the orbital momentum connected with rotation of a third cluster around center of mass of two-cluster subsystem.

To solve correctly the three-cluster problems, we need to solve two-cluster Schrödinger equation for three different two-cluster partitions α ($\alpha = 1, 2, 3$). Energy of two-cluster bound states determine the threshold energy of two-body channels and wave functions determine an asymptotic form of three-body functions in the part of coordinate space which Faddeev and Merkuriev denoted as Ω_{α} (see pages 134-135 of book [7]), i.e. in the region where distance \mathbf{x}_{α} between selected pairs of clusters is much smaller that distance between other pairs of clusters ($x_{\alpha} \ll x_{\beta}$, $x_{\alpha} \ll x_{\gamma}$). Having solved the Schrödinger equations for all two-cluster subsystems, we can proceed with solving the Schrödinger equation for three-cluster system (see eq. (31) and (33) in Ref. [1]). It is well know [8] that the Schrödinger equations for two- and three-cluster systems can be reduced to two- and three-body equations, respectively, with nonlocal and energy-dependent potentials. The later needs special attention and has to taken into account. The most simple way of overcoming this problem is to use a square-integrable basis.

The essence of the model, employed in the present investigations, is to use a discretization scheme with the help of square-integrable basis. It allows us to reduce the Schrödinger equation for many-channel system to the set of algebraic equations, which can be easily solved numerically. In present model we use of the Gaussian basis to describe bound and pseudo-bound states of two-cluster subsystems, and we employ the Oscillator basis to study interaction of the third cluster with two-cluster subsystem. The explicit definition of the Gauss and oscillator basis functions, deducing of set of linear equations for wave function and boundary conditions for wave function are presented in Refs. [1, 2].

3 Results

We use two nucleon-nucleon potentials: the Minnesota potential (central components are taken from [9, 10]) and the Modified Hasegawa-Nagata potential (MHNP) [11, 12]. Oscillator length b ,

which is common for all clusters, is adopted to minimize the threshold energy of the three-cluster channel. In this way we optimize description of the internal structure of all clusters. For ${}^8\text{Li}$ (${}^8\text{B}$) and the MP it equals $b = 1.451$ fm and for MHNP it equals $b = 1.362$ fm. In present calculations, we use the Majorana parameter m of the MHNP [11, 12] and parameter u of the MP [9] as adjustable parameters. These parameters are slightly changed to reproduce the bound state energy of ${}^8\text{B}$. This is done in order to be consistent with the experimental situation in ${}^8\text{Li}$ and ${}^8\text{B}$ nuclei. In Table 1 we show spectrum of the ${}^8\text{Li}$ and ${}^8\text{B}$ bound states, which is obtained with "optimal" input parameters. Experimental data are from Ref. [13]. Energy of bound states in ${}^8\text{Li}$ and ${}^8\text{B}$ is reckoned from the two-cluster threshold ${}^7\text{Li} + n$ and ${}^8\text{Be} + n$, respectively. One can see that the MHNP provides more correct description of the bound state spectrum in ${}^8\text{Li}$. Meanwhile, the optimal input parameters of the MP leads to too very close position of the ground 2^+ state and the first excited 1^+ state.

Table 1 – Optimal input parameters and spectrum of bound states in ${}^8\text{Li}$ and ${}^8\text{B}$. Energy of the bound states is determined from the ${}^7\text{Li} + n$ and ${}^8\text{Be} + p$ thresholds in ${}^8\text{Li}$ and ${}^8\text{B}$, respectively

Nucleus	${}^8\text{Li}$			${}^8\text{B}$		
	MP	MHNP	Exp.	MP	MHNP	Exp.
b , fm	1.3451	1.3620		1.3451	1.3620	
m (u)	0.9600	0.4157		0.9600	0.4157	
J^π	E , MeV	E , MeV	E , MeV	E , MeV	E , MeV	E , MeV
2^+	-1.958	-1.908	-2.032	-0.1368	-0.1393	-0.1375
1^+	-1.607	-0.977	-1.051			

To achieve convergence of energy of the ${}^8\text{Li}$ and ${}^8\text{B}$ bound states as a function of number of the Gaussian and oscillator functions, we investigated in detail how energy of bound and resonance states depends on number of basis functions. We found that 4 Gaussian functions and 50 oscillator functions provide an acceptable precision of microscopic calculations of energy and other parameters of the bound states, such as, for instance, the root-mean-square proton, neutron and mass radii. It is also established that, 4 Gaussian functions and 130 oscillator functions guarantee a necessary precision of the scattering matrix and energy and width of resonance states calculations.

In Table 2 we display the proton, neutron and mass rms radii of the ground state in ${}^8\text{Li}$ and ${}^8\text{B}$ nuclei. Experimental data are taken from Ref. [14]. Theoretical results are in a good agreement with the experimental data. One can see that our results confirm the existence of the neutron halo in ${}^8\text{Li}$ and the proton halo in ${}^8\text{B}$, as neutron (proton) rms radius is larger than the proton (neutron) rms radius in ${}^8\text{Li}$ (${}^8\text{B}$). This is confirmed by the last column of the Table, where the difference between proton and neutron rms radii is displayed. Our results are also in a good agreement with the results, obtained in similar microscopic models [15], [16].

Table 2 – Proton (R_p), neutron (R_n) and mass (R_m) rms radii (in fm) of the ground state in ${}^8\text{Li}$ and ${}^8\text{B}$. Energy of the ground state is in MeV

	NNP	E	R_p	R_n	R_m	$ R_p - R_n $
${}^8\text{Li}$	MP	-2.001	2.174	2.516	2.394	0.342
	MHNP	-1.908	2.174	2.548	2.415	0.374
	Exp.		2.266(0.02)	2.446(0.02)	2.376(0.02)	
${}^8\text{B}$	MP	-0.137	2.724	2.217	2.546	0.507
	MHNP	-0.139	2.756	2.244	2.576	0.512
	Exp.		2.496(0.03)	2.336(0.03)	2.436(0.03)	

Let us now turn our attention to the resonance states. Resonance states in ${}^8\text{Li}$ and ${}^8\text{B}$, generated by interaction of neutron with ${}^7\text{Li}$ and proton with ${}^8\text{Be}$ respectively, are demonstrated in Table 3. Experimental parameters of resonance states are taken from Ref. [13]. As one can see energy and width of resonance states strongly depends on shape of resonance states. For instance, energy of the first 3^+ resonance state in ${}^8\text{Li}$ obtained with the MHNP

potential is 12 times larger than the one calculated with the MP, and width is almost 50 times larger than the width calculated with the MP. There is one exception, when parameters of resonance state, calculated with both potentials are very close to each other. This is the 3^+ resonance state in ${}^8\text{B}$. In this case energy and width of the resonance state do not differ so dramatically as for other resonance states.

Table 3 – Spectrum of resonance states in ${}^8\text{Li}$ and ${}^8\text{B}$. Energy of resonances is given in MeV (Theory) or in MeV \pm keV (Experiment). Theoretical and experimental width of resonance states is indicated in keV

${}^8\text{Li}$					${}^8\text{B}$				
J^π		MP	MHNP	Exp	J^π		MP	MHNP	Exp
3^+	E	0.049	0.610	0.223 ± 3	3^+	E	2.480	2.560	2.183 ± 20
	Γ	3	166	33 ± 6		Γ	495	572	350 ± 30
1^+	E	1.535	1.002	1.178	1^+	E	0.090	0.615	0.632 ± 2.5
	Γ	826	1433	≈ 1000		Γ	0.4	43.7	35.6 ± 0.6
1^+	E	4.619	2.129	3.368	1^-	E	1.441	1.132	
	Γ	22	913	≈ 650		Γ	989	1828	
3^+	E	2.458	3.625		0^+	E	1.644	1.128	
	Γ	2636	760			Γ	870	299	
4^+	E	4.486	3.190	4.498 ± 20	2^-	E	4.209	3.363	3.363 ± 500
	Γ	64	2	35 ± 15		Γ	632	4143	8000 ± 4000

Comparing theoretical and experimental parameters of resonance states, we come to the conclusion that the MHNP provides more precise description of resonance states in ${}^8\text{Li}$ and ${}^8\text{B}$ than the MP. One can see from Table 3, the energy and width of the 1^+ and 2^- resonance states in ${}^8\text{B}$ and the 1^+ resonance state in ${}^8\text{Li}$, calculated with the MHNP, are close to experimental values. However, the MP provides fairly good description of parameters of 4^+ resonance state in ${}^8\text{Li}$ and 3^+ resonance state in ${}^8\text{B}$.

The above mentioned results are obtained with taking into account the cluster polarization. To see explicitly the effects of cluster polarization, the polarizability of clusters is switched off. We demonstrate effects of the cluster polarization only for two bound states and two resonance states, determined with the MHNP. By switching off the cluster polarization in ${}^8\text{Li}$, we obtain energy of the bound states $E(2^+) = -1.25$ MeV and $E(1^+) = -0.54$ MeV, which should be compared with

$E(2^+) = -2.00$ MeV and $E(1^+) = -1.31$ MeV. As we see, the cluster polarization decreases significantly energy of the bound states in ${}^8\text{Li}$. Let us turn our attention to the resonance states. Note, that most part of resonance states in ${}^8\text{Li}$ (${}^8\text{B}$), displayed in Table 3, are determined in the ${}^7\text{Li} + n$ (${}^8\text{Be} + p$) elastic scattering. Consider the 1^+ resonance state in ${}^8\text{B}$. By neglecting the cluster polarization we obtain parameters of the resonance state: $E = 0.94$ MeV and $\Gamma = 163$ keV. Comparing these parameters with the corresponding results in Table 3, we came to the conclusion that cluster polarization decreases 1.5

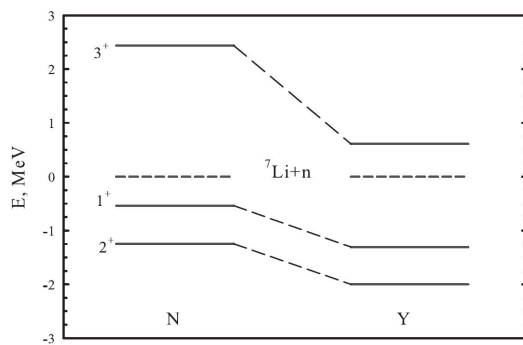


Figure 1 – Spectrum of two bound states and one resonance state in ${}^8\text{Li}$ obtained without (N) and with (Y) cluster polarization

One can see, that cluster polarization influences significantly on the phase shift of $n + {}^7\text{Li}$ scattering with the orbital momentum of neutron $l_1 = 1$. However, effects of cluster polarization on $n + {}^7\text{Li}$ scattering with $l_1 = 3$ is very small.

There is other way for visualization of cluster polarization. As was suggested in [1], by using wave function of a bound state of compound system, we can calculate how the average distance between two selected clusters depends on distance to the third cluster. For instance, we can calculate average distance between alpha particle and triton (${}^3\text{He}$) when neutron (proton) is moving toward to ${}^7\text{Li}$ (${}^7\text{Be}$). This quantity is displayed in Figure 3 for the ground 2^+ and first excited 1^+ states in ${}^8\text{Li}$. When neutron is far away from ${}^7\text{Li}$, the average distance between alpha particle and triton is approximately 4.5 fm. When neutron approach to ${}^7\text{Li}$, the average distance is reduced slightly, and then it significantly stretched when the distance $R(n - {}^7\text{Li})$ is at range between 1.5 and 9 fm. Seems, at this range nucleus ${}^7\text{Li}$ changes it

times energy and almost 4 times the total width of the 1^+ resonance state. More stronger effects of the cluster polarization is observed in the 3^+ resonance state in ${}^8\text{Li}$. Energy of the resonance state is decreased from 2.438 MeV to 0.61 MeV and width is reduced from 1227 keV to 166 keV due to the cluster polarization.

Figures 1, 2 visualize effects of cluster polarization in ${}^8\text{Li}$ and ${}^8\text{B}$. These results are obtained with the MHNP. In Figure 2, the orbital momentum l_1 denotes the orbital momentum of neutron with respect to ${}^7\text{Li}$ nucleus.

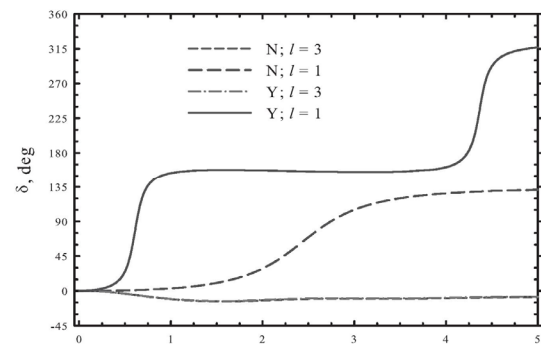


Figure 2 – Phase shifts of $n + {}^7\text{Li}$ scattering with the total angular momentum $J^\pi = 3^+$.

orientation with respect to neutron which results in such tremendous size of the system $\alpha + t$. And finally, when neutron is very close to the center of mass of ${}^7\text{Li}$ it compressed to minimal size of 1.6 fm. Thus, this figure demonstrates that ${}^7\text{Li}$ as a two-cluster system is strongly affected by incident neutron. Some what different picture is observed for the ground state of ${}^8\text{B}$. Effects of incident proton on distance between alpha particle and ${}^3\text{He}$ is demonstrated in Figure 4. The incident proton gradually decreases size of ${}^7\text{Be}$, which is due to a combination of nuclear forces and Coulomb interaction. The "phase transition", observed in bound states of ${}^8\text{Li}$ in a wide range of distance $R(n - {}^7\text{Li})$, now takes place in a very small range of $R(p - {}^7\text{Li})$ distance. However, an amplitude of the "phase transition" in ${}^8\text{B}$ is much more than in ${}^8\text{Li}$. It should be notes that without polarization, all curves in Figures and are transformed into plain lines, i.e. radius of two-cluster subsystem is independent on position of third cluster when polarization is neglected.

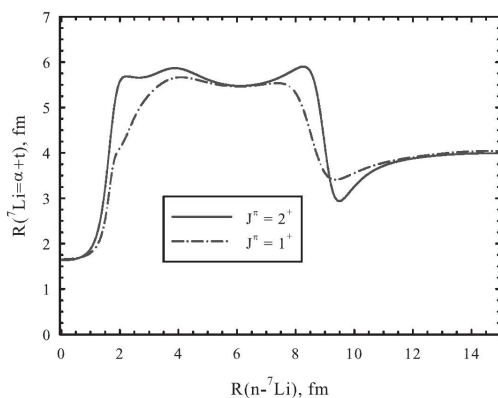


Figure 3 – Average distance between α particle and triton as a function of distance between neutron and ${}^7\text{Li}$. Calculation is made with the MHNP

We have applied a three-cluster microscopic model for studying structure of bound states and reactions in ${}^8\text{Li}$ and ${}^8\text{B}$. The model took into account polarizability of interacting clusters. It was demonstrated that the cluster polarization has large impact on properties of bound and resonance states and on the elastic scattering of neutron on ${}^7\text{Li}$ and proton on ${}^7\text{Be}$. The present model provides fairly

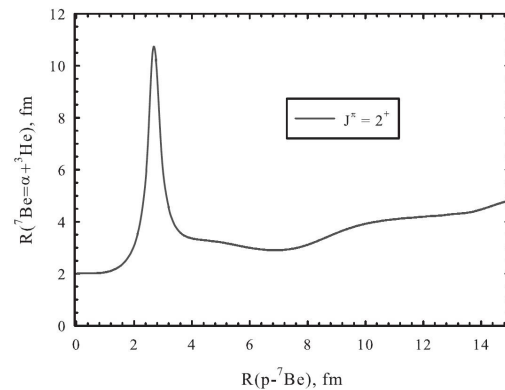


Figure 4 – Dependence of average distance between alpha particle and ${}^3\text{He}$ on distance to proton. Results are obtained with the MHNP

good description of the bound and resonance states in mirror nuclei ${}^8\text{Li}$ and ${}^8\text{B}$.

Acknowledgment

This work is partially supported by the Ministry of Education and Sciences of Republic of Kazakhstan, The Research Grant IPS 3106/GF4.

References

- [1] V. S. Vasilevsky, F. Arickx, J. Broeckhove, and T. P. Kovalenko. A microscopic three-cluster model with nuclear polarization applied to the resonances of ${}^8\text{Be}$ and the reaction ${}^6\text{Li}(p, {}^3\text{He}){}^4\text{He}$ // Nucl. Phys. A.– 2009.– Vol. 824. – P. 37–57.
- [2] A. V. Nesterov, V. S. Vasilevsky, and T. P. Kovalenko. Effect of cluster polarization on the spectrum of the ${}^7\text{Li}$ nucleus and on the reaction ${}^6\text{Li}(n, {}^3\text{H}){}^4\text{He}$ // Phys. Atom. Nucl.– 2009. – Vol. 72. – P. 1450–1464.
- [3] A. V. Nesterov, V. S. Vasilevsky, and T. P. Kovalenko. Microscopic model of the radiative capture reactions with cluster polarizability. Application to ${}^8\text{Be}$ and ${}^7\text{Li}$ // Ukr. J. Phys. – 2011.– Vol. 56. – P. 645–653.
- [4] V. S. Vasilevsky, A. V. Nesterov, and T. P. Kovalenko. Three-cluster model of radiative capture reactions in seven-nucleon systems. Effects of cluster polarization // Phys. Atom. Nucl. – 2012. – P. 75. 818–831.
- [5] J. P. Mitchell, G. V. Rogachev, at el. Low-lying states in ${}^8\text{B}$ // Phys. Rev. C.– 2010. – Vol. 82. – P. 011601.
- [6] J. P. Mitchell, G. V. Rogachev, at el. Structure of ${}^8\text{B}$ from elastic and inelastic ${}^7\text{Be}+p$ scattering // Phys. Rev. C. – 2013. – Vol. 87. – P. 054617.
- [7] L. D. Faddeev and S. P. Merkuriev. Quantum Scattering Theory for Several Particle Systems // Dordrecht, Boston, London: Kluwer Academic Publishers. – 1993.
- [8] K. Wildermuth and Y. Tang. A unified theory of the nucleus. Braunschweig: Vieweg Verlag. – 1977.
- [9] D. R. Thompson, M. LeMere, and Y. C. Tang. Systematic investigation of scattering problems with the resonating-group method // Nucl. Phys. A. – 1977. – Vol. 286. – P. 53–66.
- [10] I. Reichstein and Y. C. Tang. Study of $N + \alpha$ system with the resonating-group method // Nucl. Phys. A.– 1970. – Vol. 158. – P. 529–545.
- [11] A. Hasegawa and S. Nagata. Ground state of ${}^8\text{Li}$ // Prog. Theor. Phys.– 1971.– Vol. 45. – P. 1786–1807.
- [12] F. Tanabe, A. Tohsaki, and R. Tamagaki. $\alpha\alpha$ scattering at intermediate energies // Prog. Theor. Phys. – 1975. – Vol. 53. – P. 677–691.
- [13] D. R. Tilley, J. H. Kelley, at el. Energy levels of light nuclei $A=8, 9, 10$ // Nucl. Phys. A. – 2004. – Vol. 745. – P. 155–362.
- [14] M. M. Obuti, T. Kobayashi, at el. Interaction cross section and interaction radius of the ${}^8\text{B}$ nucleus // Nucl. Phys. A. – 1996.–Vol. 609. – P74–90.
- [15] A. Csoto. Proton skin of ${}^8\text{B}$ in a microscopic model // Phys. Lett. B. – 1993. – Vol. 315. – P. 24–28.
- [16] D. Baye, P. Descouvemont, and N. K. Timofeyuk. Matter densities of ${}^8\text{B}$ and ${}^8\text{Li}$ in a microscopic cluster model and the proton-halo problem of ${}^8\text{B}$ // Nucl. Phys. A. – 1994. – Vol 577. – P. 624–640.